Applied Science and Engineering Progress, Vol. 13, No. 4, pp. 354–361, 2020

Research Article

Simulation of Die-swell Flow for Wet Powder Mass Extrusion in Pharmaceutical Process

Vimolrat Ngamaramvaranggul*
Department of Mathematics and Computer Science, Faculty of Science, Chulalongkorn University, Bangkok, Thailand

Nawalax Thongjub
Department of Mathematics and Statistics, Faculty of Science and Technology, Thammasat University, Pathumthani, Thailand

* Corresponding author. E-mail: vimolrat.n@chula.ac.th DOI: 10.14416/j.asep.2020.03.004
Received: 1 October 2019; Revised: 1 December 2019; Accepted: 24 January 2020; Published online: 11 March 2020
© 2020 King Mongkut's University of Technology North Bangkok. All Rights Reserved.

Abstract
The simulation of extrusion spheronization in pharmaceutical industry is constructed to develop drug product. This process has four steps: mixing, extrusion, spheronization and drying. The mixing combines water and powder together with high shear until it creates strong bonds to gather powder particles in liquid solution. The work is focused on extrusion of wet powder masses, which can be classified as non-Newtonian fluid. The continuous creeping flow motion is explained in terms of the Navier-stokes equation and the rheological behavior is represented by Oldroyd-B constitutive model. The solution is solved with numerical scheme through the semi-implicit Taylor-Galerkin/pressure-correction finite element method in two-dimensional axisymmetric system under the conditions of isothermal, incompressible, laminar flows. In addition, the velocity gradient recovery and the streamline-upwind/Petrov-Galerkin schemes are applied to improve the convergence of solution. Finally, the swelling ratio of extruded product is presented to compare with the experimental results in drug production. The extrudate size obtained from computation shows agreement with both the experiment and the analytical figures. The extrudate size for experiment matches well with computational method with a discrepancy to the analytical formula. The swelling ratio of free surface for experiment is slightly different from numerical prediction with an error of 1% whilst the error between analytical and experimental values reaches 6%. For the next simulation to duplicate the feasible products, the new setting can be checked by this simulation before the set-up of real experiment.

Keywords: Extrusion spheronization, Pharmaceutical process, Semi-implicit Taylor-Galerkin finite element method, Die-swell, Oldroyd-B fluid

1 Introduction

In the early 1960s an extrusion-spheronization technique [1], [2] was developed into four standard processes to produce identical shapes with the same size as spheroids and this process is used in the pharmaceutical factory in order to make granules denser for solid oral dosage forms with minimum specific quantity of excipients. The names of these four systematic series are mixing, extrusion, spheronization and drying processes as shown in Figure 1. The powder mixing process is mixing water and powder together under shear stress to make solid network bonds and the way how to prepare pellets is described in [3]. The wet

Please cite this article as: V. Ngamaramvaranggul and N. Thongjub, "Simulation of die-swell flow for wet powder mass extrusion in pharmaceutical process," *Applied Science and Engineering Progress*, vol. 13, no. 4, pp. 354–361, Oct.–Dec. 2020.

powder mass extrusion is set to form a raw material under expel through small dies similar to sieve and give the outcome of rod style. Spheronization is a rapid step to adjust the products become spheroids or pellets. The simulation is determined in process of extrusion especially the small region before die and a bit over die exit. The function of extrusion process is imitated close to real event around extruder so as to gain the maximum profit that can give more products at short time and by product of the way how to choose proper controlled conditions for preproduction before advancing to the actual work in the real world. The die-swell problem in extrusion process [4] is widely found in many manufacturing technology not only in the pharmaceutical drugs but also in polymer melt industries and agribusiness. In the manufacture of drugs, extrusion is applied to produce various sizes of granules and pellets for convenient delivery system. There are many types of extruders such as screw extruders, gravity-fed extruders, ram extruder, roll extruder, and screen or basket extruder. For the process of extrusion, raw materials are pumped under control at high pressure and temperature passing a heated barrel to construct uniform shape and density [5], [6]. The preproduction is set as mathematical models to describe the motion of wet powder mass and a numerical method is taken to solve instead of analytical scheme since it is not too complicated to get the answer and then the solution will be the guideline to make us know that whether all adjusted conditions are accurate enough for real production. The flow behavior of material before extrusion is simulated with nonlinear partial differential equations and the solver can be finite element method (FEM), finite volume method (FVM) and finite difference method (FDM). One popular method is used to evaluate such a problem of die-swell for slit, circular, and annular dies for Newtonian and Maxwell fluids is FEM [7]. To make the extrudate more precisely, some researchers add slip condition on die wall [8], [9] or some determine thermal impacts on free surface shape [10]. Before the complex problem is computed, the simple algorithm should be prepared to make sure that the solution is good enough. The common simulation of the first starting is the stick-slip problem in Newtonian fluid without gravity and then moving on to die-swell problem [11]. The predictions of the flow behavior at free surface paths for viscoelastic fluids depend on constitutive model such as power law [12], Maxwell, Oldroyd-B [13], [14], and Phan-Thien/Tanner [15], [16] etc.

In this research, the effect of the swelling extrusion is concerned in drug manufacturing, especially in the step of transformation from the wet powder masses to pellets. The two dimensional axisymmetric flows under the isothermal circumstances are considered. The flow motion is derived from the conservation of mass and momentum that are the continuity and Navier-stokes equations including flow behavior via constitutive equation that is presented in terms of Oldroyd-B model. All mathematical models are nonlinear differential equations that are solved by the semi-implicit Taylor-Galerkin/pressure-correction finite element method. For each time step the velocity gradient recovery is selected to stabilize the converging solutions with no-slip condition. The swelling ratio of this problem is compared with the experiment in drug field.

2 Material and Method

The equipments for four processes of extrusion spheronization in pharmaceutical industry are the processes of mixing, extrusion, spheronization and drying as shown in Figure 1(a)–(d). The wet powder masses for this research are the mixture as Figure 1(a) of microcrystalline cellulose, lactose, and water with the ratio of 1:1:1.3. Before the last process, the screw expels the paste passes through the die plate of extruder as in Figure 1(b). All the extrudates in Figure 1(c) are cut by rotating friction plate while all small rods are transformed to spheres. After spheronization process, the spheroids or pellets are died in a, for example, fluidized bed dryer. The Figure 2(a)–(c), the products of each step in the extrusion process, are wet powder mass, extrudates and spheroids respectively.

3 Governing Equations

Since the wet powder masses have many network bonds that show viscous and elastic properties same as viscoelastic fluid, the flow behaviors may be described by Oldroyd-B constitutive model. To observe material discharge trajectory in isothermal condition, two models that are obtained from conservation of mass and momentum are employed to represent the liquid incompressibility under creeping motion. The derived

(a) mixing

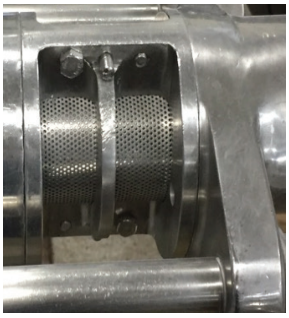

(b) extrusion

(c) spheronization

(d) drying

Figure 1: The equipment of extrusion/spheronization process.

(a) wet powder mass

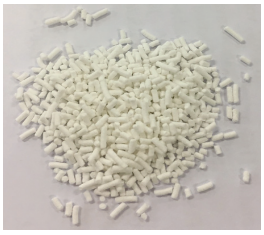

(b) extrudates

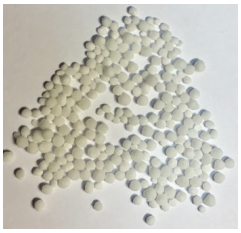

(c) spheroids

Figure 2: The product of extrusion/spheronization process.

expressions are Equations (1) and (2).

For the continuity equation, the differential form is the velocity divergence

$$\nabla \cdot \boldsymbol{u} = 0 \tag{1}$$

where $\boldsymbol{u}$ is the velocity vector and ∇ is the differential operator.

In case of the non-linear differential Navier-Stokes equation, the model is the relation between density (ρ), pressure (p), extra-stress tensor ($\boldsymbol{T}$) and time (t) as shown in Equations (2).

$$\rho \frac{\partial \boldsymbol{u}}{\partial t} = \nabla \cdot \boldsymbol{T} - \rho \boldsymbol{u} \cdot \nabla \boldsymbol{u} - \nabla p \tag{2}$$

For convenience to compare the size of extrudate with real experiment, all models are converted to non-dimensional system. After transformation, it is found that Equation (1) gives the same expression whilst Equation (2) provides similar model but changes the density to the Reynolds number (Re), which is a ratio of the inertial to viscous forces, as seen in Equation (3).

$$Re \frac{\partial \boldsymbol{u}}{\partial t} = \nabla \cdot \boldsymbol{T} - Re\ \boldsymbol{u} \cdot \nabla \boldsymbol{u} - \nabla p \tag{3}$$

where Re is a dimensionless value and $Re = \frac{\rho v l}{\mu_0}$, v is characteristic velocity, l is characteristic length, μ_0 is the zero-shear viscosity which is the combination of paste viscosity (μ_p) and the solvent viscosity (μ_s).

Due to the nature of material after mixing process, wet powder masses display the character of semi solid and since it contains a litter of water, the flow moves slightly as if it is in creeping motion. However, in such a fluid high viscous forces are dominant over the than advective inertial forces. In addition, the flow behavior depends on shear models e.g., the Newtonian model as follows [Equation (4)]:

$$\boldsymbol{T} = \boldsymbol{\tau} + 2\mu_p \boldsymbol{D}. \tag{4}$$

The extra-stress tensor ($\boldsymbol{T}$) is related to the paste stress tensor ($\boldsymbol{\tau}$) and the rate of deformation tensor ($\boldsymbol{D}$) as

$\boldsymbol{D} = \frac{\nabla \boldsymbol{u} + (\nabla \boldsymbol{u})^t}{2}$, where $(\ )^t$ is the transpose operator.

This simulation adopts the Oldroyd-B model in terms of non-dimensionless quantities as Equation (5).

$$We\boldsymbol{\tau}_t = 2\mu_p \boldsymbol{D} - \boldsymbol{\tau} + We(\boldsymbol{\tau} \cdot \nabla \boldsymbol{u} + (\nabla \boldsymbol{u})^t \cdot \boldsymbol{\tau} - \boldsymbol{u} \cdot \nabla \boldsymbol{\tau}) \tag{5}$$

where the non-dimensional Weissenberg number (We)

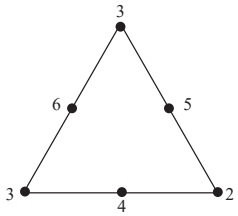

Figure 3: Triangular element shape.

equals $\frac{\lambda_1 v}{l}$, where λ_1 is the relaxation time and τ_t is time derivative of τ.

The Navier-stokes Equation (3) is solved with semi-implicit Taylor-Galerkin pressure-correction method (STGFEM). The equation is split in three simple expressions which are termed fractional steps. The first and last formulas embed the unknown of velocity but the middle step goes for the pressure variable.

3.1 *Semi-implicit Taylor-Galerkin pressure-correction finite element method*

In this research, we consider finite element method for the two dimensional triangular shape. Each element has three vertex- and three midside-nodes as shown in Figure 3. The triangular element shape functions are created into 2 types, that are linear triangular element shape functions for pressure and quadratic triangular element shape functions for velocity and stresses.

The three fractional steps are derived from the Taylor-Galerkin scheme by expanding the time derivative term with Taylor series and spatial derivative term with Galerkin finite element method. Furthermore, the first step to compute velocity contains a semi-implicit treatment which provides two half-time steps and the pressure from mid-way stage is put to correct the velocity at the final operation. The domain network is generated into small triangular bias mesh. The three fractional steps per time step are:

Step 1a: The half- time step of velocities and stresses can be derived from the equations below [Equations (6) and (7)]:

$$\left(2\frac{Re}{\Delta t}\right)(\boldsymbol{u}^{n+\frac{1}{2}}-\boldsymbol{u}^{n})=\nabla\cdot\mu_s(\boldsymbol{D}^{n+\frac{1}{2}}-\boldsymbol{D}^{n})$$
$$+\left(\nabla\cdot(\boldsymbol{\tau}+2\mu_s\boldsymbol{D})-Re\,\boldsymbol{u}\cdot\nabla\boldsymbol{u}-\nabla p\right)^{n} \quad (6)$$

$$\left(2\frac{We}{\Delta t}\right)(\boldsymbol{\tau}^{n+\frac{1}{2}}-\boldsymbol{\tau}^{n})=(2\mu_s\boldsymbol{D}-\boldsymbol{\tau})^{n}$$
$$+We\left(\boldsymbol{\tau}\cdot\nabla\boldsymbol{u}+(\nabla\boldsymbol{u})^{t}\cdot\boldsymbol{\tau}-\boldsymbol{u}\cdot\nabla\boldsymbol{\tau}\right)^{n} \quad (7)$$

Step 1b: The transient stage of intermediate velocities and a full time step of stresses are updated as in the following Equations (8) and (9):

$$\left(\frac{Re}{\Delta t}\right)(\boldsymbol{u}^{*}-\boldsymbol{u}^{n})=(\nabla\cdot\boldsymbol{\tau}-\mathrm{Re}\,\boldsymbol{u}\cdot\nabla\boldsymbol{u})^{n+\frac{1}{2}}$$
$$+\nabla\cdot\mu_s(\boldsymbol{D}^{*}-\boldsymbol{D}^{n})+2\mu_s\nabla\cdot\boldsymbol{D}^{n}-\nabla p^{n} \quad (8)$$

$$\left(\frac{We}{\Delta t}\right)\left(\boldsymbol{\tau}^{n+1}-\boldsymbol{\tau}^{n}\right)=\left(2\mu_p\,\boldsymbol{D}-\boldsymbol{\tau}\right)^{n+\frac{1}{2}}$$
$$+We\,(\boldsymbol{\tau}\cdot\nabla\boldsymbol{u}+(\nabla\boldsymbol{u})^{t}\cdot\boldsymbol{\tau}-\boldsymbol{u}\cdot\nabla\boldsymbol{\tau})^{n+\frac{1}{2}} \quad (9)$$

Step 2: Full time step of pressure is related to velocity according to the equation.

$$\nabla^2(p^{n+1}-p^{n})=\left(\frac{2\,Re}{\Delta t}\right)\nabla\boldsymbol{u}^{*} \quad (10)$$

Step 3: Solve full time step velocities [Equation (11)]:

$$\left(\frac{2Re}{\Delta t}\right)(\boldsymbol{u}^{n+1}-\boldsymbol{u}^{*})=\nabla(p^{n+1}-p^{n}) \quad (11)$$

The velocity vector of steps 1 and 3 are calculated via the Jacobi iteration method while the pressure is computed in step 2 with the Cholesky decomposition scheme. After complete calculation for equation of motion, the techniques of the velocity gradient recovery and streamline-upwind/Petrov-Galerkin are applied to force the stability outcome.

3.2 *Theoretical prediction*

This simulation is created to gain a size of extrudate from numerical solution that is close to real product by adjusting material parameters until the magnitude of imitation is equivalent to real dimension. One important scale to measure the product is the swelling

ratio χ of die radius (R_j) to extrudate radius (R) or in notation $\chi = \frac{R_j}{R}$. The swelling ratio of elastic fluid for the theoretical predictions as proposed by Tanner [17] is [Equation (12)]:

$$\chi = 0.13 + \left(1 + 0.5S_r^2\right)^{\frac{1}{6}} \quad (12)$$

where, S_r is recovery shear and $S_r = \frac{N_1}{2\tau_{rz}}$, N_1 is the first normal stress difference and τ_{rz} is the shear stress. For a Poiseuille entry flow of wet powder mass via Oldroyd-B model, $S_r = \beta We$ and $\beta = \frac{\mu_p}{\mu_0}$.

4 Problem Specification

Experimental data in unit measurement has the following details. Density (ρ) of wet powder mass is 0.821 g/cm^3. Plug velocity (V_{plug}) at boundary x_3x_4 is 0.39 mm/s. Pipe length (x_1x_2) is 1 mm. Die radius (R_j or x_2x_5) is 1 mm. Extrudate radius (R or x_3x_4) is the average value from quadruple measurements, that are 1.084, 1.153, 1.342 and 1.451 mm so the mean radius value is 1.258 mm. Zero-shear viscosity (μ_0) of wet powder mass is 89 g/cm·s. Relaxation time (λ_1) is 0.998 s. Suppose that entrant flow has the parabolic shape of $V_{max}\left(1 - \frac{r^2}{R_i^2}\right)$ then take V_{plug} from tryout measurement to calculate maximum velocity at inlet under conservation of flowrate (Q).

$$Q_{inlet} = 2\pi \int_0^{R_j} rV_{max}\left(1 - \frac{r^2}{R_i^2}\right)dr$$

$$= 2\pi V_{max} \int_0^1 r(1 - r^2)dr$$

$$= \frac{1}{2}\pi V_{max}$$

$$Q_{outlet} = \pi r^2 V_{plug} = \pi(1)^2(0.39) = 0.39\pi$$

From conservation of flowrate, inlet flowrate equals outlet flowrate that is $\frac{1}{2}\pi V_{max} = 0.39\pi$. So we get V_{max} = 0.78 mm/s.

Numerical mesh data and boundary conditions are exhibited in Figures 4 and 5. The stick-slip domain as shown in Figure 4(a) is generated to small finite triangular meshes with 2052 elements and 4255 nodes the same as die-swell shape as in Figure 4(b) as the size of extrudate is calculated from stick-slip problem by direct insertion of slip velocity on top free surface after die-exit. The non-dimensional values are as the following: V_{max} = 1, x_1x_2 = 1, x_2x_3 = 2, x_1x_6 = 1. The ratio of paste viscosity (μ_p) to the solvent viscosity μ_s is 0.95:0.05. To find the non-dimensional numbers of *Re* and *We*, the maximum velocity at inlet and die radius are taken as the characteristic length and velocity so

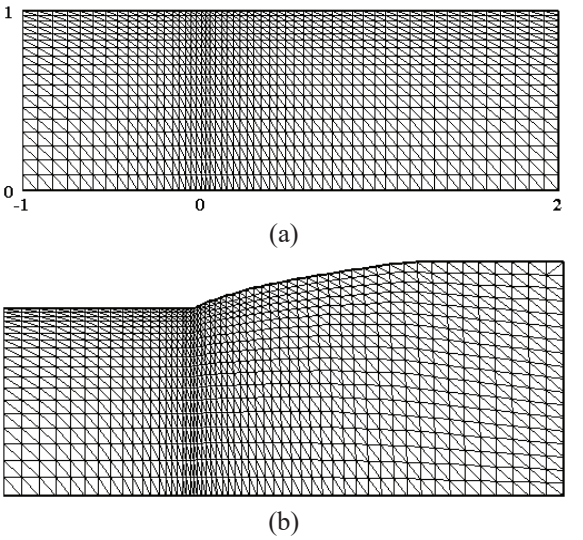

Figure 4: (a) Stick slip domain (b) Die swell geometry.

$$Re = \frac{(0.821g/cm^3)(0.78\,mm/s)(1\,mm)}{89g/cm \cdot s}$$

$$= 7.195 \times 10^{-5}$$

and $We = \frac{(0.998s)(0.78\,mm/s)}{1\,mm} = 0.778.$

So, swelling ratio for theoretical prediction is:

$$\chi = 0.13 + \left(1 + 0.5\left[\frac{\mu_p}{\mu_0}We\right]^2\right)^{\frac{1}{6}}$$

$$= 0.13 + \left(1 + 0.5[0.95 \times 0.778]^2\right)^{\frac{1}{6}} = 1.171$$

The boundary conditions for die-swell flow as in Figure 5 are set as Poiseuille flow, that velocity profile

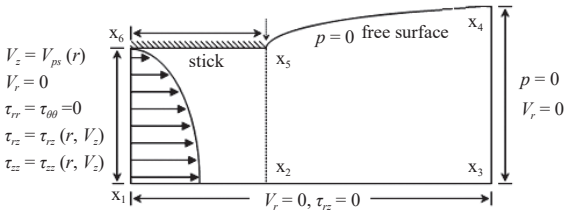

Figure 5: Boundary conditions of die swell flow.

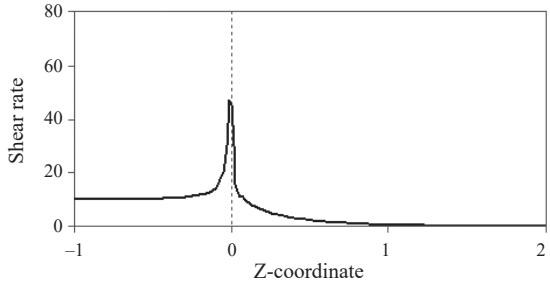

Figure 6: Shear rate on top surface.

is a parabolic curve for the axial velocity V_z at the inlet within axisymmetric coordinate system and still retains the parabolic shape while the radial velocity V_r is null at the symmetrical line.

The inlet boundary values are $V_z(r) = 1 - r^2$, $\tau_{rr} = 0$, $\tau_{\theta\theta} = 0$, $\tau_{zz} = 2We\mu_p\left(\frac{\partial V_z}{\partial r}\right)^2$, $\tau_{rz} = \mu_p\frac{\partial V_z}{\partial r}$ and the boundary conditions at symmetric line are $V_r = 0$ and $\tau_{rz} = 0$.

5 Results and Discussion

The calculation of die-swell problem is started after the convergence solution of stick-slip flow has been recorded since the stick-slip condition is a specific case study for extrudate swell under fixed geometry to bound the surface tension.

The half simple symmetric domain of stick-slip flow in Figure 3 is manipulated and then the final solution is transferred to die-swell problem in order to reset data for initial condition. The routine in complex flow program begins with the same boundary conditions except top surface of downstream section that is swapped from stick to slip velocity for adjusting free surface path. Consequently, the prediction for die-swell curve of Oldroyd-B fluid is depicted in Figure 4. The simulation of die-swell problem is evaluated with STGFEM and the solution is calculated in terms of swelling ratio (χ), normal stress (τ_{rr}, $\tau_{\theta\theta}$, r_{zz}) and shear stress (τ_{rz}). In Figure 4, the swelling ratio of computation is 1.247 along the exit of top free surface and the extrudate magnitude will be higher if the Weissenberg number rises. For this result, the largest height of streamline corresponds to theoretical prediction that is shown in Equation (10). The values of swelling ratio from computation are slightly shifted from experiment that is revealed in Table 1 with the error percentage of 1% while the analytical prediction is different from experiment with the error of 6%. The values of stresses and shear rate are measured for maximum peak at die-exit whilst pressure drop (Δp) shows the difference between entrance boundaries and die exit region on account of the pressure lost with the value of 23.71 as shown in Table 2 and Figure 7(c). The behavior of flow under shear for Oldroyd-B fluid displays the effect of shear rate and shear stress due to the sudden change in boundary among stick and slip regions. Both values generate similar curves for the same trend on the top surface as shown in Figure 6 and the maximum shear rate is 46.92. From Figure 7, the peak values of radial velocity as in Figure 7(a) is 0.22, which is very small although there is a bit swell after die but it still bears no significance. The axial velocity of Figure 7(b) is the main speed to push fluid forward as straight line due to laminar flow and the parabola curve of V_z at inlet line is developed to plug flow with the same magnitude of 0.3 at the right end boundary. The circumferential stress $\tau_{\theta\theta}$ as in Figure 7(d) has maxima at die exit on top surface with the value of 6.87 since the streamlines are extruded to free boundary. The top values of shear stress τ_{rz} and axial stress τ_{zz} in Figure 7(e) and (f) are observed around joint region and their values are 6.16 and 13.60, respectively. The stress $\tau_{\theta\theta}$ is the highest value when compared with other stresses in consideration of laminar flow at the axial direction. The streamline function of Figure 7(g) shows the line contour when the flow passes inlet to the downstream and then the stream path displays the swell line.

Table 1: The comparison of swelling ratio for various methods

	Expeiment	Theory	Computation
χ	1.258	1.171	1.247

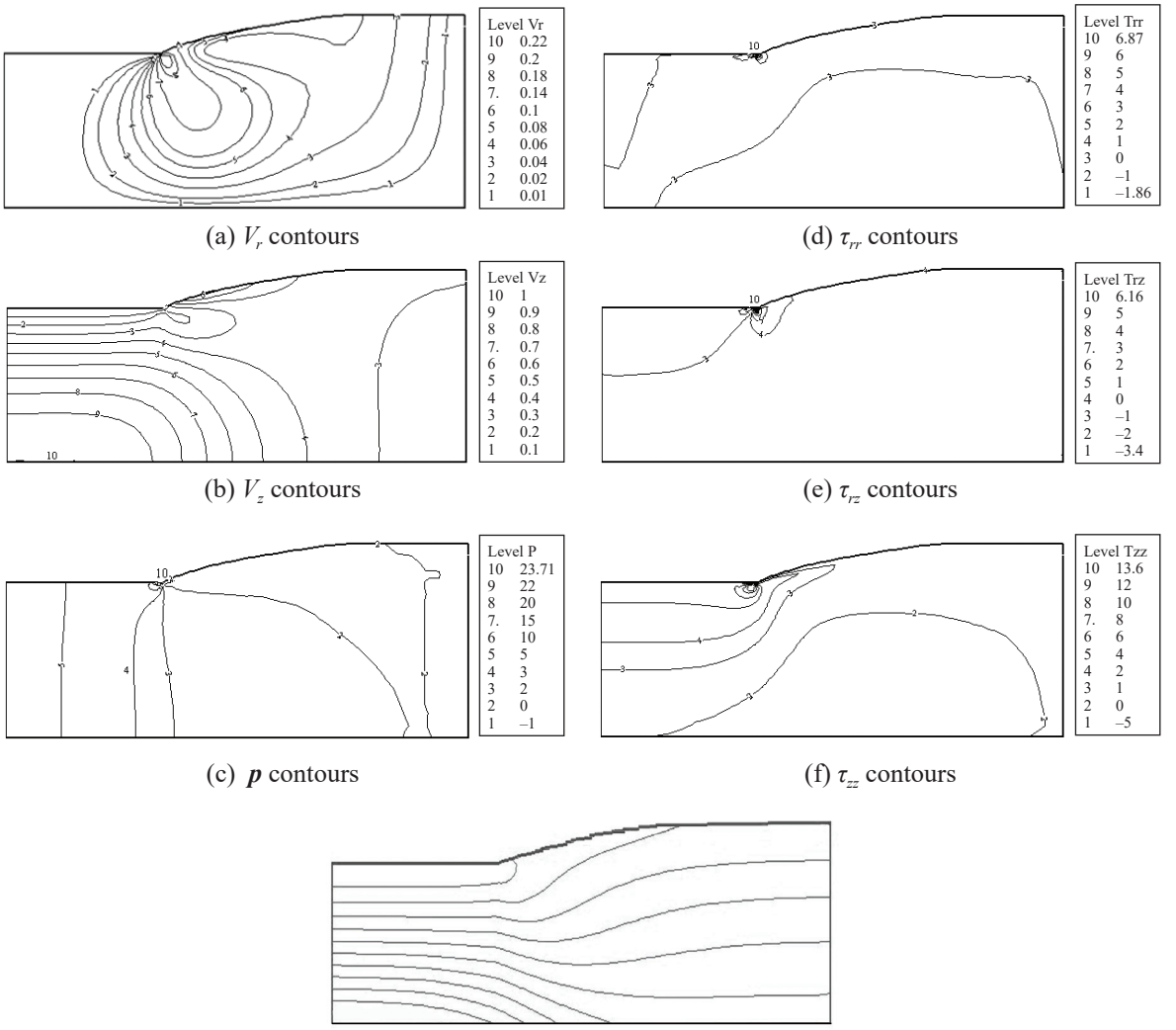

(a) V_r contours (d) τ_{rr} contours

(b) V_z contours (e) τ_{rz} contours

(c) $\boldsymbol{p}$ contours (f) τ_{zz} contours

(g) streamline contours

Figure 7: Line contours of die swell.

Table 2: The numerical result of Wet Powder Process

	Maximum	**Minimum**
V_r	0.22	0.00
V_z	1.00	0.00
τ_{rr}	6.87	–1.86
τ_{rz}	6.16	–3.40
τ_{zz}	13.60	–5.00
$\tau_{\theta\theta}$	0.55	0.10
$\Delta\boldsymbol{p}$	23.71	

6 Conclusions

The simulation under the process of extrusion for extrusion spheronization in pharmaceutical industry is set up to learn the flow behavior and find out some material parameters which match well with this experiment. The stress equation is tracked closely with natural phenomenon via Oldroyd-B model and the Navier-Stokes equation is the standard representation for streamline motion. The problem is set for incompressible die-swell flow of two dimensional axisymmetric system under isothermal condition. The result is

calculated by semi-implicit Taylor-Galerkin pressure-correction finite element method simultaneously with velocity gradient recovery and the streamline-upwind/ Petrov-Galerkin techniques. The extrudate size for experiment matches well with computational method but demonstrates difference with analytical formula. The swelling ratio of free surface for experiment is slightly different from numerical prediction with the error of 1% deviation whilst the error between analytical and experimental value is 6%. The analytical prediction from Tanner's model, that is the well know model, is applied to predict the swelling ratio for general elastic fluid but from our numerical process, we integrated three boundary conditions in order to get streamline free surface method so it is approaching to real problem. For the next simulation to duplicate the feasible products, the new setting can be checked by this simulation before the set-up of real experiment.

References

[1] C. Vervaet, L. Baert, and J. P. Remon, "Extrusion-spheronisation A literature review," *International Journal of Pharmaceutics*, vol. 116, no. 2, pp. 131–146, 1995.

[2] S. Muley, T. Nandgude, and S. Poddar, "Extrusion–spheronization a promising pelletization technique: In-depth review," *Asian Journal of Pharmaceutical Sciences*, vol. 11, no. 6, pp. 684–699, 2016.

[3] J. Chatchawalsaisin, P. Podczeck, and J. M. Newton, "The preparation by extrusion/spheronization and the properties of pellets containing drugs, microcrystalline cellulose and glyceryl monostearate," *European Journal of Pharmaceutical Sciences*, vol. 24, pp. 35–48, 2005.

[4] J. Thiry, F. Krier, and B. Evrard, "A review of pharmaceutical extrusion: Critical process parameters and scaling-up," *International Journal of Pharmaceutics*, vol. 479, pp. 227–240, 2015.

[5] J. Breitenbach, "Melt extrusion: From process to drug delivery technology," *European Journal of Pharmaceutics and Biopharmaceutics*, vol. 54, no. 2, pp. 107–117, 2002.

[6] M. Maniruzzaman, J. S. Boateng, M. J. Snowden, and D. Douroumis, "A review of hot-melt extrusion: Process technology to pharmaceutical products," *ISRN Pharmaceutics*, vol. 2012, pp. 1–9, 2012.

[7] M. J. Crochet and R. Keunings, "Die swell of a maxwell fluid numerical prediction," *Journal of Non-Newtonian Fluid Mechanics*, vol. 7, pp. 199–212, 1980.

[8] W. J. Silliman and L. E. Scriven, "Separating flow near a static contact line: Slip at a wall and shape of a free surface," *Journal of Computational Physics*, vol. 34, no. 3, pp. 287–313, 1980.

[9] N. Phan-Thien, "Influence of wall slip on extrudate swell: A boundary element investigation," *Journal of Non-Newtonian Fluid Mechanics*, vol. 26, pp. 327–340, 1988.

[10] A. Karagiannis, A. N. Hrymak, and J. Vlachopoulos, "Three-dimensional nonisothermal extrusion flows," *Rheologica Acta*, vol. 28, pp. 121–133, 1989.

[11] V. Ngamaramvaranggul and M. F. Webster, "Viscoelastic simulation of stick-slip and die swell flows," *International Journal for Numerical Methods in Fluids*, vol. 36, pp. 539–595, 2001.

[12] S. J. Chapman, A. D. Fitt, and C. P. Please, "Extrusion of power-law shear-thinning fluids with small exponent," *International Journal of Non-Linear Mechanics*, vol. 32, no. 1, pp. 187–199, 1997.

[13] N. Thongjub, B. Puangkird, and V. Ngamaramvaranggul, "Simulation of slip effects with 4:1 contraction flow for Oldroyd-B fluid," *Asian International Journal of Science and Technology in Production and Manufacturing Engineering*, vol. 6, no. 3, pp. 19–28, 2013.

[14] N. Thongjub and V. Ngamaramvaranggul, "Simulation of die-swell flow for Oldroyd-B model with feedback semi-implicit Taylor Galerkin finite element method," *KMUTNB International Journal of Applied Science Technology*, vol. 8, no. 1, pp. 55–63, 2015.

[15] V. Ngamaramvaranggul and M. F. Webster, "Simulation of pressure-tooling wire-coating flow with Phan-Thien/Tanner models," *International Journal for Numerical Methods in Fluids*, vol. 38, pp. 677–710, 2002.

[16] V. Ngamaramvaranggul and S. Thenissara, "The contraction point for Phan-Thien/Tanner model of tube-tooling wire-coating flow," *International journal of Physical and Mathematical Science*, vol. 4, no. 4, pp. 627–631, 2010.

[17] R. I. Tanner, "A theory of die swell," *Journal of Polymer Science Part A-2*, vol. 8, no. 12, pp. 2067–2078, 1970.